Reproductive Tissues Maintain Insulin Sensitivity in Diet-Induced Obesity

Sheng Wu, Sara Divall, Fredric Wondisford, and Andrew Wolfe

Reproductive dysfunction is associated with obesity. We previously showed that female mice with diet-induced obesity (DIO) exhibit infertility and thus serve as a model of human polycystic ovary syndrome (PCOS). We postulated that differential insulin signaling of tissues leads to reproductive dysfunction; therefore, a comparison of insulin signaling in reproductive tissues and energy storage tissues was performed. Pituitary-specific insulin receptor knockout mice were used as controls. High-fat diet–induced stress, which leads to insulin resistance, was also investigated by assaying macrophage infiltration and phosphorylated Jun NH_2-terminal kinase (pJNK) signaling. In lean mice, reproductive tissues exhibited reduced sensitivity to insulin compared with peripheral metabolic tissues. However, in obese mice, where metabolic tissues exhibited insulin resistance, the pituitary and ovary maintained insulin sensitivity. Pituitaries responded to insulin through insulin receptor substrate (IRS)2 but not IRS1, whereas in the ovary, both IRS1 and IRS2 were activated by insulin. Macrophage infiltration and pJNK signaling were not increased in the pituitary or ovary of lean mice relative to DIO mice. The lack of inflammation and cytokine signaling in the pituitary and ovary in DIO mice compared with lean mice may be one of the reasons that these tissues remained insulin sensitive. Retained sensitivity of the pituitary and ovary to insulin may contribute to the pathophysiology of PCOS. ***Diabetes*** **61:114–123, 2012**

Secretion of luteinizing hormone and follicle-stimulating hormone stimulates the maturation, development, and function of the gonads and, ultimately, through regulation of gonadal steroid hormone secretion, regulates reproduction. While nutritional deprivation inhibits reproductive function, it is becoming clear that nutritional excess can also impair reproductive function. Recently, the response of the reproductive axis to nutritional excess has gained attention because of the rise in obesity and its associated diseases, such as type 2 diabetes, metabolic syndrome, and polycystic ovary syndrome (PCOS) (1), all of which are associated with reproductive dysfunction. PCOS is defined as hyperandrogenism with oligo/amenorrhea and accounts for >75% of cases of anovulatory infertility. PCOS is marked by an increase in luteinizing hormone pulsatility, often accompanied by high baseline luteinizing hormone levels, ovarian overproduction of testosterone, polycystic ovaries, and peripheral insulin resistance. The pathophysiologic mechanisms underlying the reproductive and metabolic derangements in PCOS have yet to be delineated. We recently revealed a role for insulin signaling in the pituitary in a mouse model of obesity-induced reproductive dysfunction and hyperandrogenism (2).

While insulin resistance in the energy-storing tissues has been extensively studied, the effects of chronic hyperinsulinemia and obesity in tissues of the female reproductive axis have been more superficially addressed. Analysis of the insulin receptor substrate (IRS)2 knockout (KO) mouse has confirmed the importance of the IRS2 scaffolding protein for normal reproductive function (3); yet, the role that IRS1 and -2 play in the function of reproductive tissues in obesity has not been explored. Therefore, an analysis of the insulin-signaling pathways in the pituitary and ovary in lean and diet-induced obesity (DIO) mice was performed in this study. We demonstrate that the mechanisms that induce insulin resistance at the level of IRS2 are absent in the pituitary and ovary and that retained insulin sensitivity in reproductive tissues results in elevated insulin signaling in hyperinsulinemic conditions such as obesity.

RESEARCH DESIGN AND METHODS

Animals and diets. Mice were maintained on a mixed background: CD1/129SvJ/C57BL6. Pituitary-specific insulin receptor KO mice (PITIRKO) were produced by our group as described previously (2). αGSU-Cre-negative littermates were used as controls (wild type [WT]). Female PITIRKO mice and controls were fed a high-fat diet (HFD) or regular chow as described previously (2). Mice used in this study were female and were maintained with food and water ad libitum under a 14-h/10-h dark/light cycle. Procedures were approved by the Johns Hopkins Animal Care and Use Committee. Experiments were conducted with 5.5- to 6.5-month-old female mice (lean and DIO): lean WT (30.6 ± 1.0 g), lean PITIRKO (29.6 ± 1.8 g), WT DIO (44.3 ± 6.9 g), and PITIRKO-DIO (43.4 ± 6.4 g). Mice were tested for estrous cyclicity, and WT DIO mice were acyclic as reported previously (2).

Hormonal assays. Mice were fasted overnight, and blood was collected from mice via mandibular bleed at 10 A.M. All samples were collected by 10:30 A.M. Insulin, leptin, and glucagon were measured with the Milliplex Map Mouse Serum Adipokine Panel (Millipore, Billerica, MA), and insulin-like growth factor-I (IGF-I) was measured with a single-plex IGF-I panel (Millipore) on a Luminex 200IS platform (Luminex Corporation, Austin, TX). All samples were performed in one plate. The intra-assay coefficient of variation for each assay was between 5 and 9%.

Glucose and insulin tolerance tests. Mice were fasted overnight and injected intraperitoneally with 2 g/kg body wt dextrose. Glucose was measured from tail blood at the times indicated using a One Touch Ultra glucometer. After insulin injection (Lilly, Indianapolis, IN) in lean and WT DIO mice, glucose was measured as described above.

Insulin-signaling assay. Mice were fasted overnight, and insulin or 0.9% saline was injected intraperitoneally with different doses. Tissues were collected at 10, 15, 30, or 45 min after insulin injection and snap-frozen in liquid nitrogen. Protein was obtained and measured as described previously (2). To quantify the levels of phosphorylated AKT (pAKT), phosphorylated extracellular signal–related kinase (pERK), and AKT for different tissues of each individual animal after insulin or saline injection, Bio-Plex Phosphoprotein Detection Multiplex assays were used (Bio-Rad Laboratories, Hercules, CA. For quantification of phosphorylated Tyr (pTyr)-IRS1 (or total IRS1) levels in cell lysates, Milliplex Map Phospho IRS1 Mapmates (or Total IRS1 Mapmates) kits were used. Protein (10 μg) from each tissue was loaded into a 96-well microplate. Tissues from four to eight mice were measured independently and were not

From the Department of Pediatrics, Johns Hopkins University School of Medicine, Baltimore, Maryland.
Corresponding author: Sheng Wu, swu24@jhmi.edu.
Received 10 July 2011 and accepted 11 October 2011.
DOI: 10.2337/db11-0956
This article contains Supplementary Data online at http://diabetes.diabetesjournals.org/lookup/suppl/doi:10.2337/db11-0956/-/DC1.

pooled. Assays were conducted using the Luminex 200 system. Values were assessed as mean fluorescent intensity. For quantification of the pTyr-IRS2 level, a PathScan Phospho-IRS-2 (panTyr) ELISA kit (Cell Signaling Technology) was applied according to the manufacturer's instructions.

Antibodies and immunoblotting. Identical amounts of protein were loaded and separated by SDS-PAGE gel and blotted onto nitrocellulose membranes. Signals were detected by enhanced chemiluminescence plus Western Blotting Detection System (GE Healthcare, Buckinghamshire, U.K.). Rabbit primary antibodies against pAKT (Ser473), AKT, pERK, ERK, phosphorylated Jun NH_2-terminal kinase (pJNK), Jun NH_2-terminal kinase (JNK), and actin were from Cell Signaling Technology. Rabbit anti-IRS1 was from Millipore. Goat anti-rabbit IgG (H+L)-HRP conjugate was from Bio-Rad Laboratories.

Total RNA extraction, reverse transcription, and quantitative PCR. Pituitary and ovary RNA was extracted and reverse transcribed as previously described (4). For the expression of *irs1*, iQ SYBR Green quantitative PCR (Bio-Rad Laboratories) was performed, and *irs1* primers were from the study by Murata et al. (5). *gapdh* was used as described previously (4). *irs1* values were corrected with *gapdh* values. Reactions were performed using an iCycler iQ5 quantitative PCR machine (Bio-Rad Laboratories) as described previously (4).

Immunohistochemistry. Tissues were paraffin sectioned by Johns Hopkins University Pathology Core Facility. Sections were stained with rat anti-mouse F4/80 (1:100) and Mac-2 (1:200), and markers for macrophages (6) were purchased from Cedarlane (Burlington, Ontario, Canada). Secondary antibody Alexa Fluor 594 goat anti-rat IgG (H+L) (1:200) was from Invitrogen.

Statistical analysis. All data were analyzed with unpaired two-tailed Student *t* test using Prism Software (GraphPad Software, Inc.) and are expressed as means ± SEM. $P < 0.05$ was defined as statistically significant.

RESULTS

DIO mice exhibit insulin resistance. We measured fasting serum insulin, leptin, glucagon, and IGF-I levels in mice fed an HFD and in chow-fed control littermates. Insulin and leptin levels were elevated in DIO mice relative to controls as reported previously (Fig. 1*A* and *B*) (2,7). DIO mice had lower serum glucagon levels than did controls (Fig. 1*C*); IGF-I levels were unchanged in DIO mice relative to those in lean controls. (Fig. 1*D*). DIO mice exhibited glucose intolerance after D-dextrose injection in as little as 15 min (Fig. 1*E*).

Blood glucose levels after insulin injection. We measured the time course of the response of circulating glucose levels to insulin in order to identify a time at which we could measure early insulin-signaling events independent of insulin-induced hypoglycemia. We injected overnight-fasted lean mice with insulin (0.5, 1, 1.5, and 3 units/kg body wt) and measured glucose at 10, 30, and 45 min after injection. Glucose levels declined, as expected, at the 30- and 45-min time points for all doses of insulin. No significant decrease in glucose levels was observed at 10 min for any of the doses of insulin (Fig. 2). Additionally, the highest levels of pAKT in the pituitary and ovary were observed at this time (Supplementary Fig. 1). Therefore, for all subsequent studies (except those specifically addressed) a 10-min time point was used to avoid the effects of hypoglycemia on signaling pathway activity.

Pituitary and ovary are less insulin sensitive than classic energy storage tissues. For determination of whether reproductive tissues (hypothalamus, pituitary, and ovary) are comparable in insulin sensitivity with classical energy storage tissues such as liver, muscle, and fat, insulin (0.5, 1, or 1.5 units/kg body wt) was injected intraperitoneally into fasted lean WT female mice. At 10 min, tissues were collected, and pAKT, pERK, and total AKT levels were quantified by Luminex assays. Results are expressed as fold change compared with data from saline-injected littermates. Liver and muscle showed significantly increased pAKT levels at 0.5 units/kg body wt insulin (Fig. 3*A* and *C*), demonstrating that intraperitoneal insulin administration achieves circulating insulin levels at 10 min adequate for inducing signaling

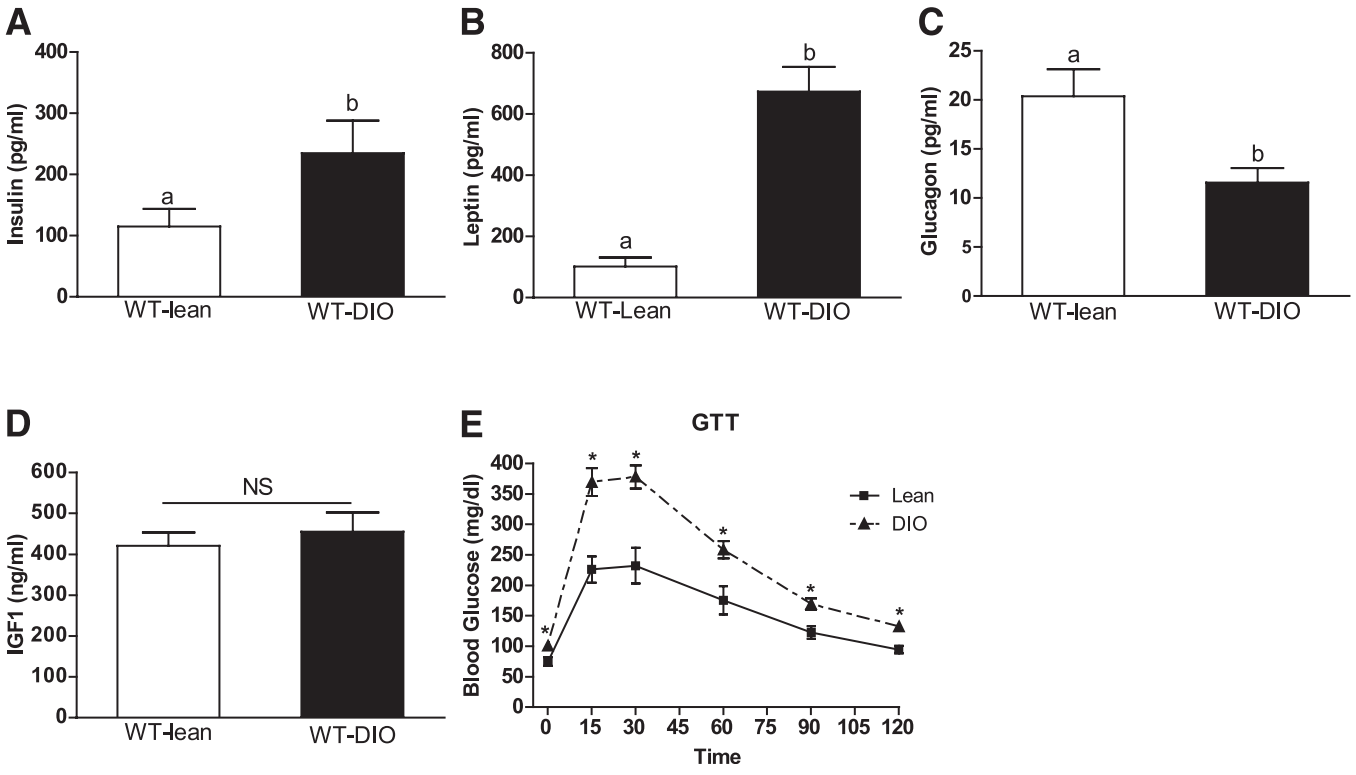

FIG. 1. WT lean and DIO female mice were fasted overnight, and biochemical data are shown. *A*: Insulin. *B*: Leptin. *C*: Glucagon. *D*: IGF-I. *E*: Glucose tolerance test (2 g/kg i.p. D-glucose injected; glucose levels measured at different time points). *n* = 4–6/group. *,[a,b]Significant differences ($P < 0.05$). NS, nonsignificant. GTT, glucose tolerance test.

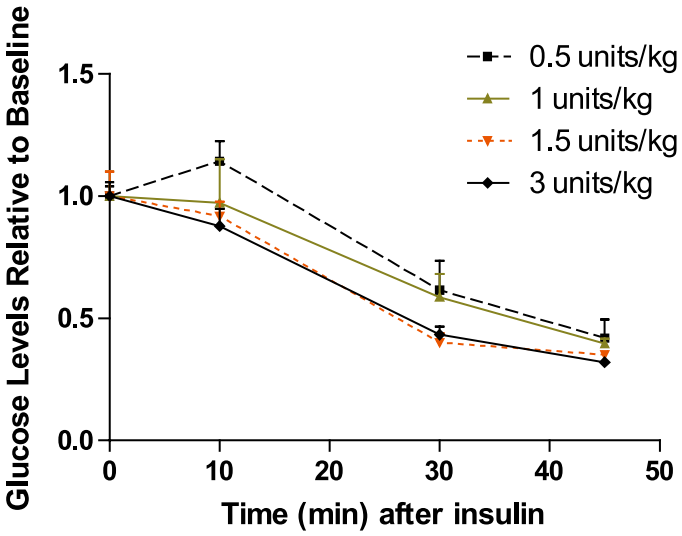

FIG. 2. Time course of response to different doses of insulin in overnight-fasted lean female mice. Glucose was measured at 0, 10, 30, and 45 min. No significant decline in glucose levels was observed at any dose at 10 min. (A high-quality color representation of this figure is available in the online issue.)

in these tissues. However, the pituitary and ovary first demonstrated AKT phosphorylation at the higher insulin dose of 1.5 units/kg body wt (Fig. 3*E* and *G*). No change in pAKT levels was observed in the hypothalamus at any of the doses (Fig. 3*I*). There was no significant increase in pERK in pituitary, ovary, or hypothalamus in response to insulin (Fig. 3*F*, *H*, and *J*). Muscle and liver exhibited increased pERK levels at 1 and 1.5 units/kg body wt insulin but not 0.5 units/kg body wt insulin (Fig. 3*B* and *D*). Because no changes in ERK signaling were observed in the reproductive tissues at these doses, subsequent analyses focused on changes in the phosphatidylinositol (PI) 3-kinase signaling pathway. Meanwhile, total AKT levels were also measured, with no observed difference between insulin- and vehicle-injected lean mice (Fig. 3*K*, *L*, and *M*).

In addition to Luminex assays of insulin signaling, we conducted Western blot analysis to explore insulin-signaling pathways in reproductive tissues and the energy storage tissues (Fig. 4*A*). We found similar tissue-specific phosphorylation patterns in response to insulin using Western blot analysis. We analyzed insulin signaling in the DIO mice by Western blot, and both the pituitary and ovary responded to insulin with increased phosphorylation of AKT. Furthermore, higher basal levels of pAKT were observed in the pituitary and ovary of DIO female mice compared with those in lean WT mice (Fig. 4*B*). However, insulin resistance was clearly observed in liver in DIO mice with dramatic reduction in the levels of insulin-stimulated pAKT compared with those seen in lean mice (Fig. 4*B*).

Pituitary and ovary express higher basal levels of pAKT and maintain insulin sensitivity in WT DIO mice. Although pituitary and ovary were less sensitive to insulin than muscle and liver, we observed that they maintain insulin sensitivity in obese mice in which insulin resistance was demonstrated in the energy storage tissues. To examine the differences between the tissues in pAKT signaling with higher throughput, accuracy, and sensitivity, we used four to eight animals per tissue per treatment and applied each individual protein into 96-well microplates to perform Luminex signaling assays. Since AKT phosphorylation in the reproductive tissues only increased at higher insulin doses in the lean mice, 3 units/kg body wt insulin were also included in our study. Pituitary-specific insulin receptor conditional KO mice were examined as a control to verify that the pAKT signaling is mediated through the insulin receptor. After 12 weeks of HFD, WT DIO mice showed a blunted response to insulin in liver and muscle compared with that in the lean WT mice (Fig. 5). Basal levels of pAKT in the pituitary and ovary were also significantly elevated in DIO mice relative to lean mice, and insulin treatment increased levels of pAKT to equal magnitudes in both lean and DIO mice (Fig. 5*A* and *B*). The increased basal level of pAKT and the response to insulin in pituitary were confirmed to be mediated by the insulin receptor by using PITIRKO-DIO mice that had no significant increase of basal or insulin-stimulated pAKT levels in the pituitary relative to lean mice. Since the insulin receptor is intact in the liver, muscle, and ovary, these tissues respond to insulin nearly identically to WT DIO mice (Fig. 5*B*, *D*, and *E*). The hypothalamus did not respond to insulin at even the 3 units/kg body wt dose (Fig. 5*C*).

Pituitary and ovary have tissue-specific differences in insulin signaling through the IRS proteins. IRS1 and IRS2 are scaffolding proteins that transduce signals from the insulin receptor to the PI 3-kinase and mitogen-activated protein kinase (MAPK) signaling pathways. They are also proposed as loci of protein modifications that produce insulin resistance (8). pTyr is a marker of insulin sensitivity (9), and pTyr-IRS1 levels were measured. We observed that pituitary pTyr-IRS1 levels do not change in response to insulin treatment in either lean or DIO mice (Fig. 6*A*). As for pAKT, the basal levels of pTyr-IRS1 in the ovary are elevated in DIO mice relative to those in lean mice (Fig. 6*B*). Additionally, insulin stimulated an increase in pTyr-IRS1 in the ovary in both lean and DIO mice in a dose-dependent manner. Liver and muscle exhibited insulin resistance at the level of IRS1 in DIO mice compared with lean mice (Fig. 6*C* and *D*). The insulin receptors remained intact in the ovary, liver, and muscle in the PITIRKO mice; therefore, insulin-induced IRS1 signaling in these tissues closely resembles that seen in WT mice.

Both IRS1 and IRS2 contribute to insulin signaling in ovary. Since IRS1 does not mediate insulin signaling in the pituitary, we also measured pTyr-IRS2 levels. Both the pituitary and the ovary showed higher basal levels of pTyr-IRS2 in DIO mice compared with lean controls (Fig. 6*E* and *F*). Furthermore, pTyr-IRS2 levels were increased in both the ovary and pituitary in response to insulin in both lean and WT DIO mice. In contrast, while pTyr-IRS2 levels were increased in liver and muscle in response to insulin in lean controls, there was no increase observed in DIO mice (Fig. 6*G* and *H*). Both the basal increase in pTyr-IRS2 levels in DIO mice and the insulin-stimulated increase in pTyr-IRS2 levels were absent in the pituitaries of PITIRKO mice, confirming that both are mediated by the insulin receptor. As expected, there was no difference in the responses of WT DIO and PITIRKO-DIO mice in liver, muscle, or ovary. Since we did not observe any change in pTyr-IRS1 in pituitary but did in ovary, we examined the mRNA and protein level of IRS1 in pituitary and ovary and found that both were significantly lower in the pituitary (Fig. 6*I*–*K*).

Pituitary and ovary have no obesity-related changes in macrophage infiltration or pJNK. Others have shown that HFD increased macrophage infiltration in energy storage tissues (10,11), which can induce pJNK activation

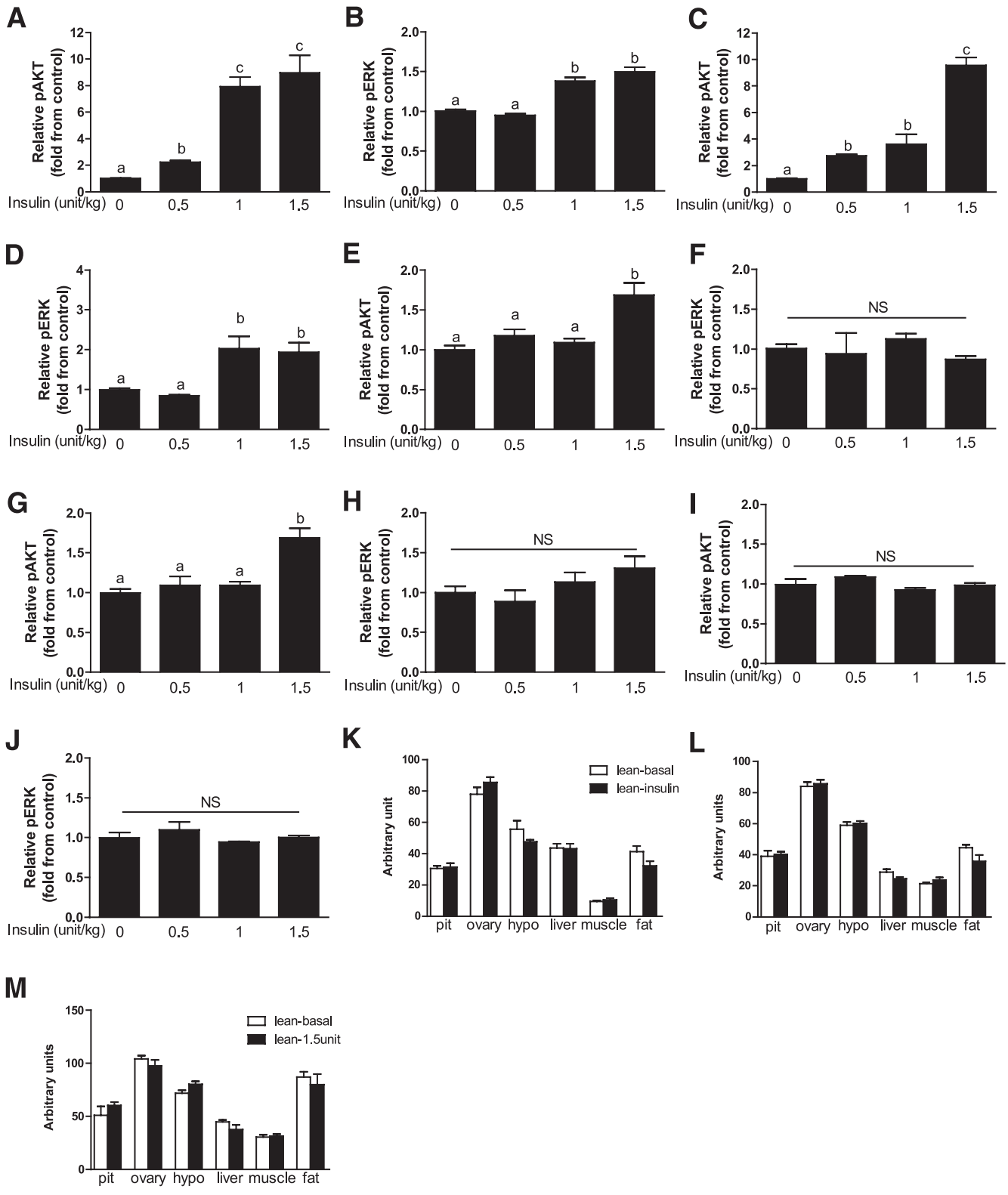

FIG. 3. Fasted lean female mice were injected with saline or 0.5, 1, or 1.5 units/kg body wt insulin, and total AKT, pAKT, and pERK1/2 levels were measured in tissue homogenates using the Luminex analyzer. pAKT and pERK values are displayed relative to those of saline-injected mice and are corrected for total AKT. Total AKT values are expressed as relative light units. Different letters indicate significant differences between groups ($P < 0.05$). *A* and *B*: Liver. *C* and *D*: Muscle. *E* and *F*: Pituitary. *G* and *H*: Ovary. *I* and *J*: Hypothalamus. *K*: 0.5 units–total AKT. *L*: 1 unit–total AKT. *M*: 1.5 units–total AKT. NS, nonsignificant. pit, pituitary. hypo, hypothalamus.

of liver and muscle in DIO mice (7,12,13). pJNK activation is a major contributor to insulin resistance (7). Since basal pAKT levels of pituitary and ovary were elevated in DIO versus lean mice, we chose to investigate whether macrophage infiltration and JNK phosphorylation were different between reproductive tissues and the energy storage tissues. Using immunofluorescence and Western blot analysis, we observed that the pituitary and ovary of

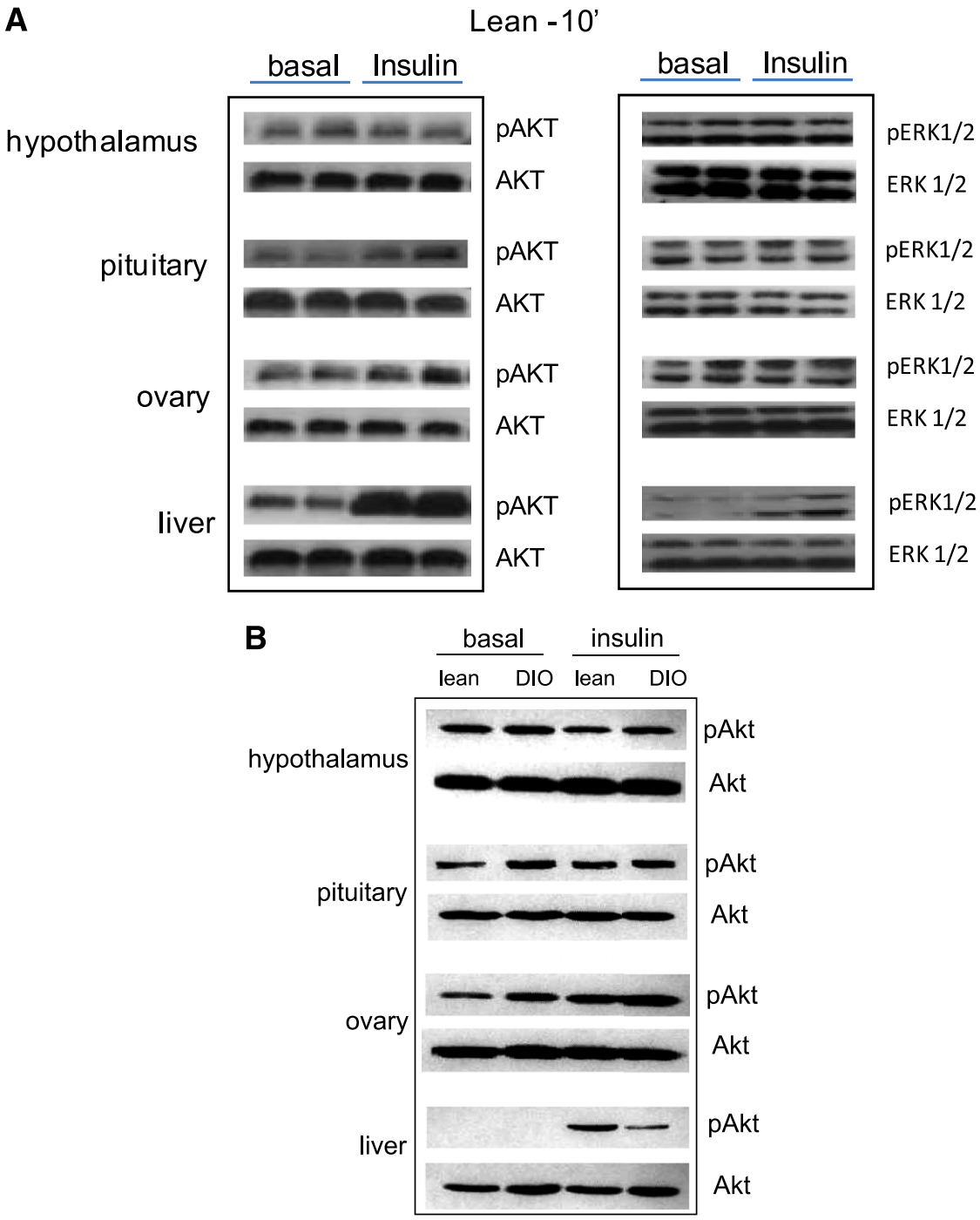

FIG. 4. Western blot identifies differences in insulin-signaling pathways between reproductive tissues and the energy storage tissues. *A*: Female lean mice were fasted overnight and injected with insulin (1.5 units/kg body wt). *B*: pAKT levels of lean and DIO female mice were compared before or after insulin stimulation. (A high-quality color representation of this figure is available in the online issue.)

DIO mice had levels of macrophage infiltration and pJNK similar to those of their lean littermates (Fig. 7*A* and *B*). In contrast, adipose tissue exhibited dramatically increased staining of the macrophage-specific protein F4/80 (Fig. 7*A*) in the DIO mice. Another macrophage-specific protein, Mac2, showed a distribution similar to that of F4/80 (data not shown). Liver and adipose tissue expressed strong staining for pJNK in the DIO mice relative to the lean controls (Fig. 7*B*). No change in total JNK was observed in examined tissues with HFD conditions (Fig. 7*B*).

DISCUSSION

That states of extreme positive energy balance and peripheral insulin resistance result in reproductive dysfunction is becoming increasingly clear. To investigate the response of reproductive tissues to hyperinsulinemia, we used a mouse model of infertility associated with DIO.

Initial analysis demonstrated that reproductive tissues required higher doses of insulin to activate downstream signaling pathways than do the classic energy storage tissues, suggesting that reproductive tissues were significantly

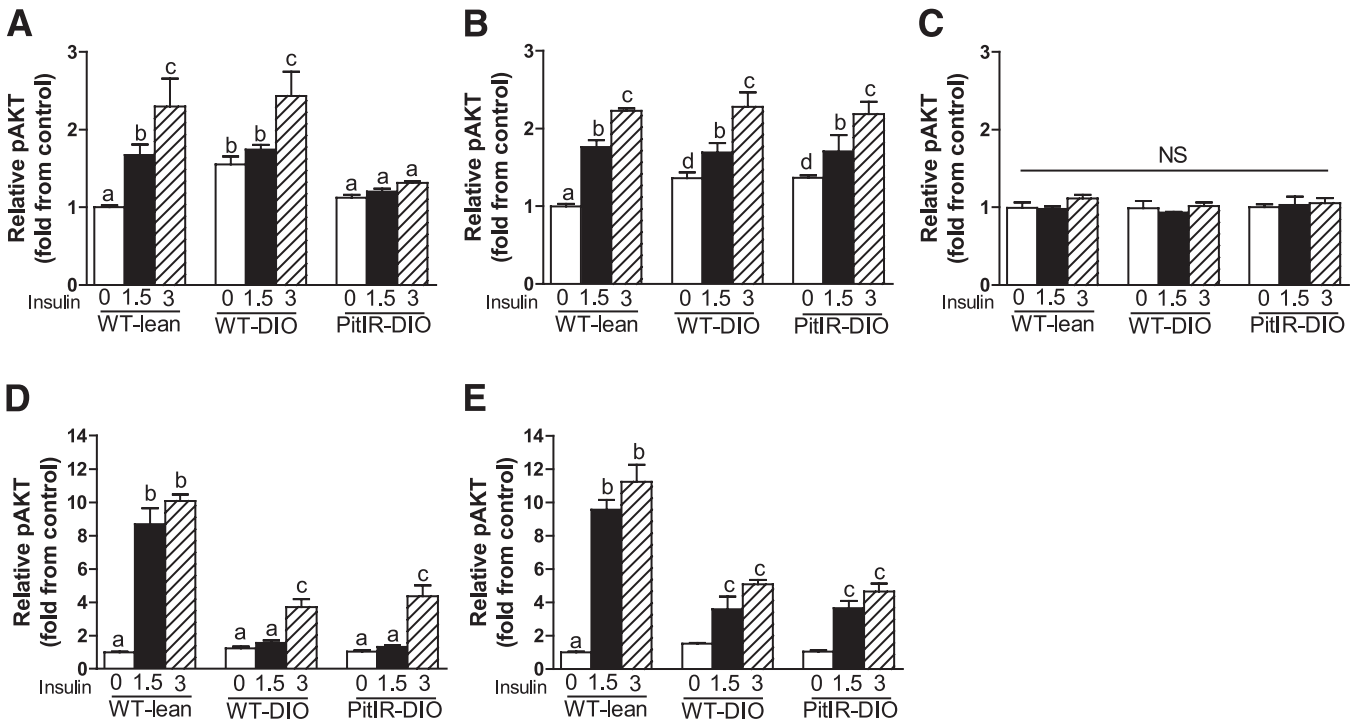

FIG. 5. Luminex analysis of pAKT signaling after overnight-fasted mice were injected with insulin. WT lean, WT DIO, and PITIRKO-DIO mice were compared with regard to reproductive and energy storage tissues. n = 4–8/group. Bars with different letters are significantly different ($P < 0.05$). *A*: Pituitary. *B*: Ovary. *C*: Hypothalamus. *D*: Liver. *E*: Muscle.

less sensitive to insulin than classical energy storage tissues (Fig. 3). These initial studies were performed in lean female mice and suggest that fundamental tissue-specific differences in insulin sensitivity exist. Under normal physiologic conditions, insulin signaling in the gonadotropin-releasing hormone neuron and pituitary does not play an important role in reproductive function, since deletion of the insulin receptor in these neurons have no impact on fertility (2,14). A role for pathologic insulin signaling in states of insulin excess could occur, however, since insulin signaling was activated in the reproductive tissues at higher doses (Fig. 3). Consistent with this assertion, mice on 60% HFD for 12 weeks develop hyperinsulinemia associated with infertility and elevated luteinizing hormone and testosterone levels (2).

Curiously, the hypothalamus exhibited no change in AKT or IRS1 phosphorylation after insulin at any time point examined (Fig. 3*I* and Supplementary Figs. 1 and 4). The hypothalamus is a putative target of insulin in feeding behavior and discrete nuclei, or whole hypothalami, as previously shown in male rats and mice, are activated by insulin (15–17). However, these studies generally used intracerebroventricular infusions of insulin or used much higher peripheral doses of insulin than were used in our studies performed in female mice. Alternatively, the effects of insulin in the hypothalamus may have been masked by an abundance of nonresponse cells in the fragment. In DIO mice, there was a blunted response to insulin signaling at the level of AKT in both liver and muscle demonstrating classical insulin resistance (Fig. 5*D* and *E*). In contrast, the pituitary and ovary exhibited elevated basal levels of pAKT and were not resistant to insulin activation of AKT in the DIO mice (Fig. 5*A* and *B*). In the pituitary, the significance of AKT activation is not known. While insulin administration causes a robust stimulation of AKT in a gonadotrope cell line (18), whether AKT signaling plays a role in luteinizing hormone secretion remains to be determined. In the ovary, AKT activation has been found to play a role in insulin induction of 5α-reductase gene expression (19) and 17α-hydroxylase activity (20), leading to an increase in ovarian androgen biosynthesis. Interestingly, polymorphisms in the *Akt2* gene have been found to be associated with PCOS in women (21). Insulin and IGF-I–induced progesterone production via MAPK pathways in the human ovary have also been described (22), with insulin stimulating the p38 family of MAPKs to induce this effect. We did not see an effect of insulin on ERK activation in the ovary but did not investigate for activation of the p38 family of MAPKs in the mice; thus, lack of activation of the entire MAPK pathway cannot be excluded by our studies.

To explore why the pituitary and the ovary maintain insulin sensitivity in the obese state, we measured activation of the IRS proteins (IRS1 and IRS2). Pituitary and ovary exhibited an elevation in basal pTyr-IRS2 levels in DIO mice compared with lean mice (Fig. 6*E* and *F*) that was similar to the tissue-specific pattern of AKT phosphorylation. In contrast with the liver and muscle, insulin was able to induce a further increase in pTyr-IRS2 levels in the pituitary and ovary from DIO mice (Fig. 6). Phosphorylation events were mediated by the insulin receptor—not the IGF-I receptor—since increases in pituitary pAKT or pTyr-IRS2 did not occur in PITIRKO mice (Figs. 5*A* and 6*E*). However, signaling characteristics in the ovary, liver, and muscle were nearly identical to those seen in WT mice. Our study is in agreement with phosphorylation patterns seen using a paradigm of chronic treatment with either insulin or human chorionic gonadotropin/insulin in rats to mimic chronic hyperinsulinemia (23,24). An increase in the IRS–PI 3-kinase/pAKT signaling pathway in whole ovary extracts was observed, while the liver and muscle became insulin

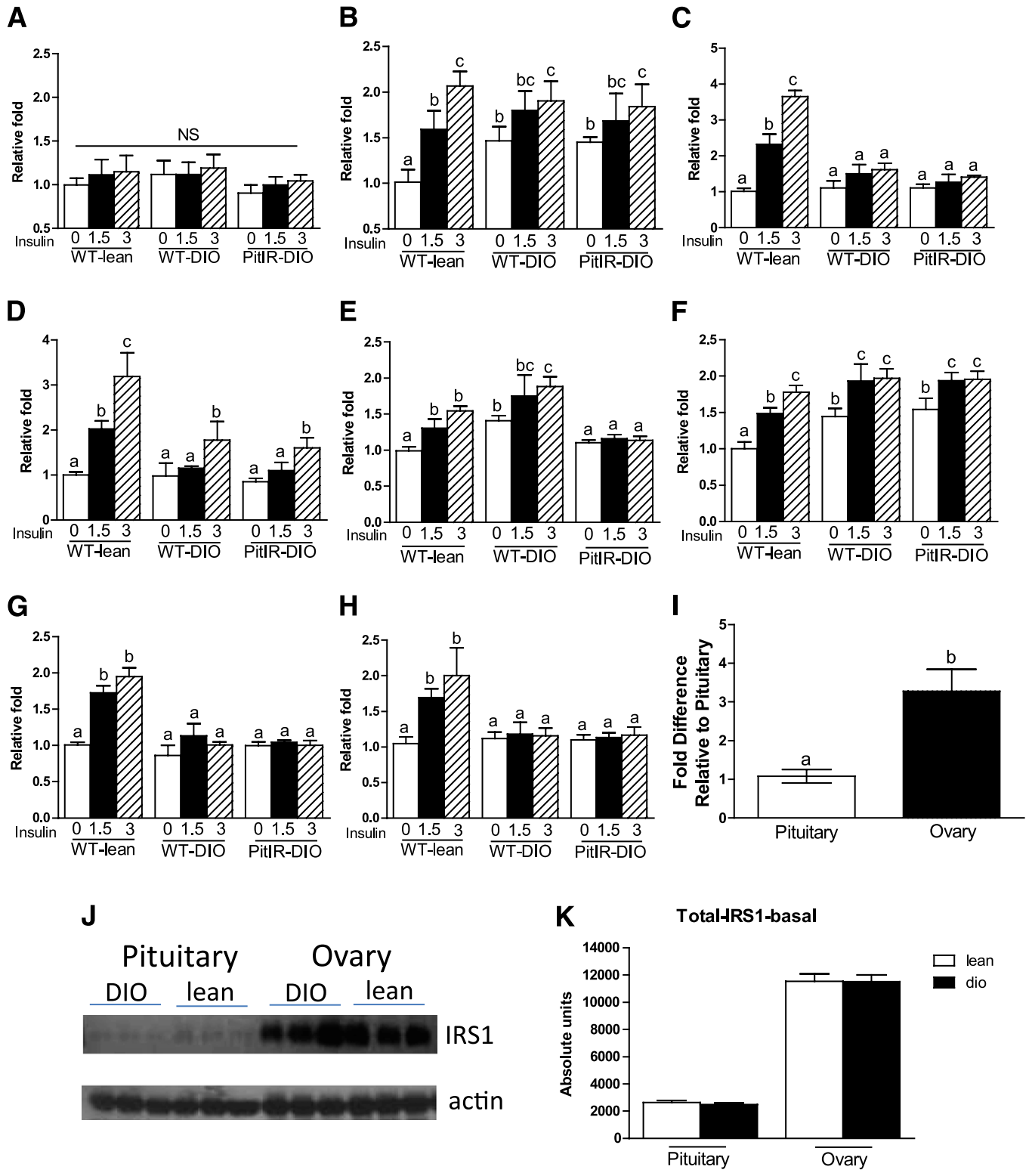

FIG. 6. Analysis of pTyr-IRS1 and pTyr-IRS2 signaling and IRS1 expression levels. *A–H*: pTyr-IRS1 (*A–D*) and pTyr-IRS2 (*E–H*) values of insulin-injected fasted mice are displayed relative to those of saline-injected mice. WT lean, WT DIO, and PITIRKO-DIO mice were compared with regard to reproductive and energy storage tissues. *n* = 4–8/group. *A* and *E*: Pituitary. *B* and *F*: Ovary. *C* and *G*: Liver. *D* and *H*: Muscle. *I*: *irs1* mRNA level was measured in pituitary and ovary by real-time PCR in fed mice. *J*: IRS1 protein level shown by Western blot. *K*: IRS1 basal protein level was measured by Luminex assay in fed mice. Bars with different letters are significantly different ($P < 0.05$). (A high-quality color representation of this figure is available in the online issue.)

resistant as indicated by attenuated insulin-induced pAKT levels. Others have reported a female rat model of hyperinsulinemia that exhibited a distinctly exhibited a distinctly PCOS appearance that was similar to our model of DIO-related infertility with high luteinizing hormone levels (23,24).

Interestingly, pTyr-IRS1 levels in the pituitary were not changed by insulin treatment in lean or DIO mice (Fig. 6*A*

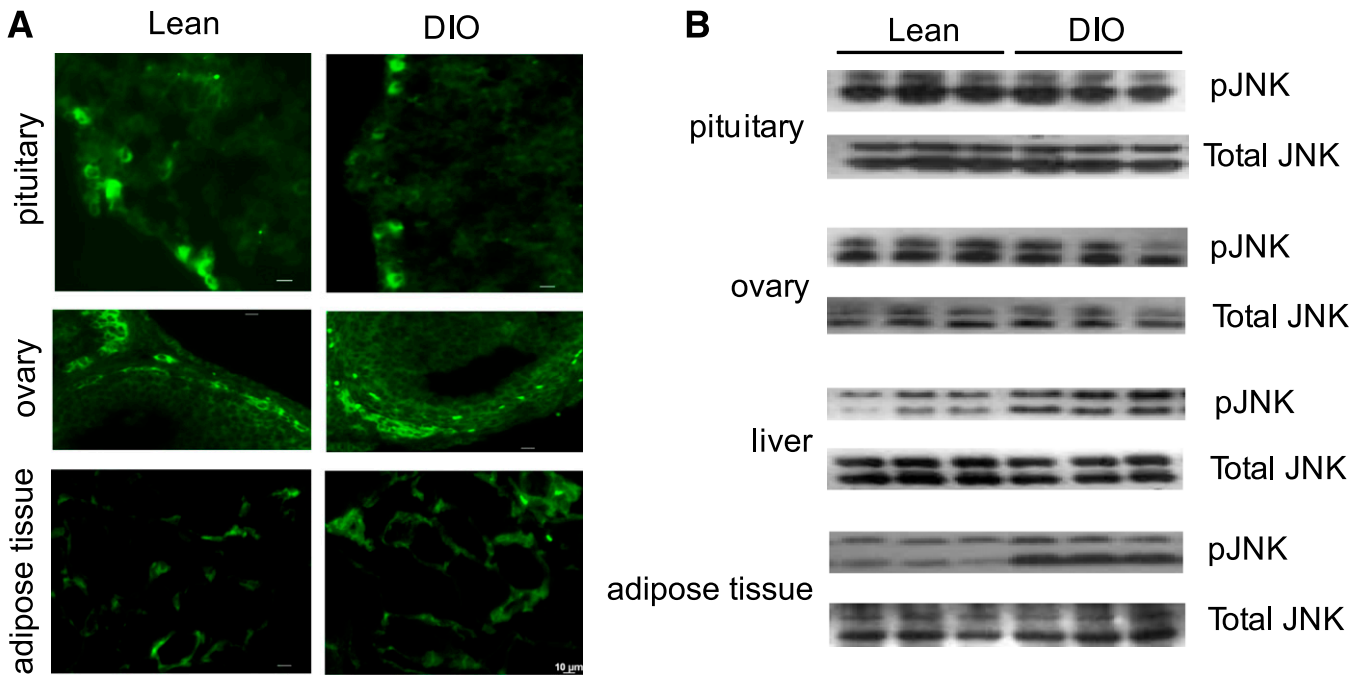

FIG. 7. HFD-induced inflammation in different tissues. *A*: Macrophage infiltration was detected by immunohistochemistry using antibody F4/80. *B*: pJNK was examined by Western blot in different tissues. (A high-quality digital representation of this figure is available in the online issue.)

and Supplementary Fig. 2), although this may be a function of the paucity of IRS1 in the pituitary as assessed by Western blot or Luminex assay (Fig. 6*I*, *J*, and *K*). Analysis of the IRS2 KO mice has also identified a similar predominant role of IRS2 in the pituitary without any detection of pTyr-IRS1 using pooled pituitaries (3). At the 10-unit dose of insulin, activation of IRS1 signaling was observed in the pituitary of both WT and PITIRKO mice, suggesting IGF-I receptor activation (Supplementary Fig. 3).

While there were significant differences in the pituitary in the phosphorylation of IRS1 and IRS2 to insulin, in the ovary, the two IRS proteins exhibited similar responses to insulin in both lean and DIO mice (Fig. 6*A*, *B*, *E*, and *F*). Insulin stimulated an increase in ovarian pTyr-IRS1 and pTyr-IRS2 in lean mice. Compared with those in lean mice, basal levels of ovarian pTyr-IRS1 and pTyr-IRS2 were elevated in DIO mice, with a further increase in levels of ovarian pTyr-IRS1 and pTyr-IRS2 after insulin administration. This preservation of insulin signaling in the setting of peripheral insulin resistance suggests that ovarian IRS is not susceptible to the mechanisms proposed to underlie tissue resistance to insulin, including serine phosphorylation and degradation of IRS (8). These data suggest that differences at this proximal level of the insulin-signaling pathway between the ovary and pituitary and the energy storage tissues underlie the retained sensitivity to insulin in obese mice.

The DIO mice are chronically hyperinsulinemic, which differs from studies that used acute or chronic insulin stimulation as a model (25,26). In the latter study, lean rats were injected with insulin for 22 days. However, these rats retained cyclicity, which may be a result of unchanged gonadotropin-releasing hormone sensitivity of the pituitary observed in this model. It is not clear whether this is a species-specific difference or due to the differences between the models of hyperinsulinemia (DIO versus insulin injection). However, recent work in a DIO rat model (27) showed that 120 days of HFD was associated with elevated circulating luteinizing hormone levels, elevated basal pAKT levels, and a retained responsiveness to acute insulin treatment—all of which were observed in our mouse DIO model (Figs. 4*B* and 5) (2). In contrast to our model, insulin resistance in the rat ovary developed after 180 days on HFD and luteinizing hormone levels normalized. The authors of the study also measured interleukin-1B, tumor necrosis factor-α, and pJNK expression in the ovary and found no increase in DIO versus lean females at 120 days but a significant increase after 180 days in DIO rats (27). These obesity-induced stress responses have been proposed as mechanisms for the development of insulin resistance in other tissues (8), and suppression of JNK signaling in liver and muscle has been shown to ameliorate insulin resistance in obese mice (28,29). The time course of cytokine expression and insulin resistance in the ovary observed by Akamine et al. (27) supports our contention that a lack of macrophage infiltration combined with a lack of increase in cytokine signaling in the pituitary and ovary may contribute to retained insulin sensitivity in the DIO mouse (Fig. 7). As our model exhibits retained insulin signaling with estrous acyclicity, this difference suggests that excessive insulin signaling may lead to anovulation and associated lack of estrous cycling. The development of ovarian insulin resistance observed by Akamine et al. may be a function of species differences (rat versus mouse). Alternatively, there are clearly time-dependent changes that occur between 120 and 180 days in the rat that could emerge with extended analysis of the DIO mice. We favor the former hypothesis, since we have observed retained insulin signaling in the ovaries and pituitaries of mice on an HFD for over 6 months (data not shown), suggesting that the protection from insulin resistance in these tissues may be more durable in the mouse than in the rat.

The lack of elevated JNK signaling in DIO mice relative to controls (Fig. 7*B*) differs from the findings of a recent

study that proposed a role for pituitary JNK signaling in the regulation of glucose homeostasis (30). These investigators noted an increase in JNK-induced c-Jun phosphorylation in DIO male mice relative to chow-fed controls. These differences are likely due to strain and sex differences between our studies.

We focused on PI 3-kinase AKT, which is thought to more closely mediate metabolic signaling, whereas the MAPK pathway mediates growth and development (31), and because our studies did not show significant changes in ERK phosphorylation between conditions. This does not preclude important roles for ERK signaling in reproductive tissues, and in fact, ERK mediates essential signaling events in both the pituitary (32) and ovary (33) as a result of G-protein receptor activation. In addition, a role for non-ERK MAPK signaling has been implicated in ovarian progesterone synthesis (22). Impaired glucose uptake and diminished accumulation of lactate were observed in granulosa cells of women with anovulatory PCOS compared with control women, suggesting that granulosa cells in women with PCOS exhibit resistance to the metabolic effects of insulin (34). While our studies did not distinguish between signaling in theca and granulosa cells, our results would be consistent with retained signaling in the theca cells. Therefore, the retained insulin responsiveness in DIO females (Figs. 5 and 6) may be manifest at the level of the theca cell even in the face of resistance in the granulosa cells, resulting in increased steroidogenesis (35–37).

Persistent ovarian sensitivity to insulin in the context of peripheral insulin resistance has been implicated in the pathophysiology of PCOS. Human studies indicate that ovarian steroidogenesis involves AKT activation (18,19) and that steroid metabolism is preserved in women with hyperinsulinemia and PCOS (2,38,39). Our results, which demonstrate maintained insulin-induced Akt phosphorylation in the ovary in the setting of hyperinsulinemia, suggest that persistent AKT phosphorylation may be contributing to the pathologic steroidogenesis in women with PCOS. Furthermore, women with type 1 diabetes, who are often treated with supraphysiologic doses of insulin on a chronic basis, have a two- to threefold increased risk of development of PCOS. It is noteworthy that this subset of women with PCOS has hyperandrogenemia, implying abnormal ovarian steroid metabolism, without evidence of elevated antimullerian hormone (produced by small ovarian follicles), luteinizing hormone-to-follicle-stimulating hormone ratio, or sulfated dihydroepiandrosterone as seen in PCOS (40).

Hence, it is likely that a hormonal milieu that differs between PCOS and type 1 diabetes is responsible for disruption of ovarian and adrenal function and that persistent AKT signaling cannot alone account for the ovarian dysfunction seen in PCOS. As a further indication of the link between hyperinsulinemia and ovarian steroidogenesis, hyperinsulinemic states induced by hyperinsulinemic-euglycemic clamps lead to increased ovarian androgen production in lean women with PCOS, demonstrating an acute induction of ovarian steroidogenesis by insulin (41).

In summary, we have shown that the insulin responsiveness of the pituitary and ovary is uniquely preserved in mice with peripheral insulin resistance (Fig. 8). Our study is the first to suggest that the preservation of insulin signaling in the pituitary and ovary of the DIO mouse occurs at a proximal point in insulin signaling, i.e., at the level of the IRS proteins. Further delineation of these pathways will provide insight into the role of hyperinsulinemia in the development of PCOS.

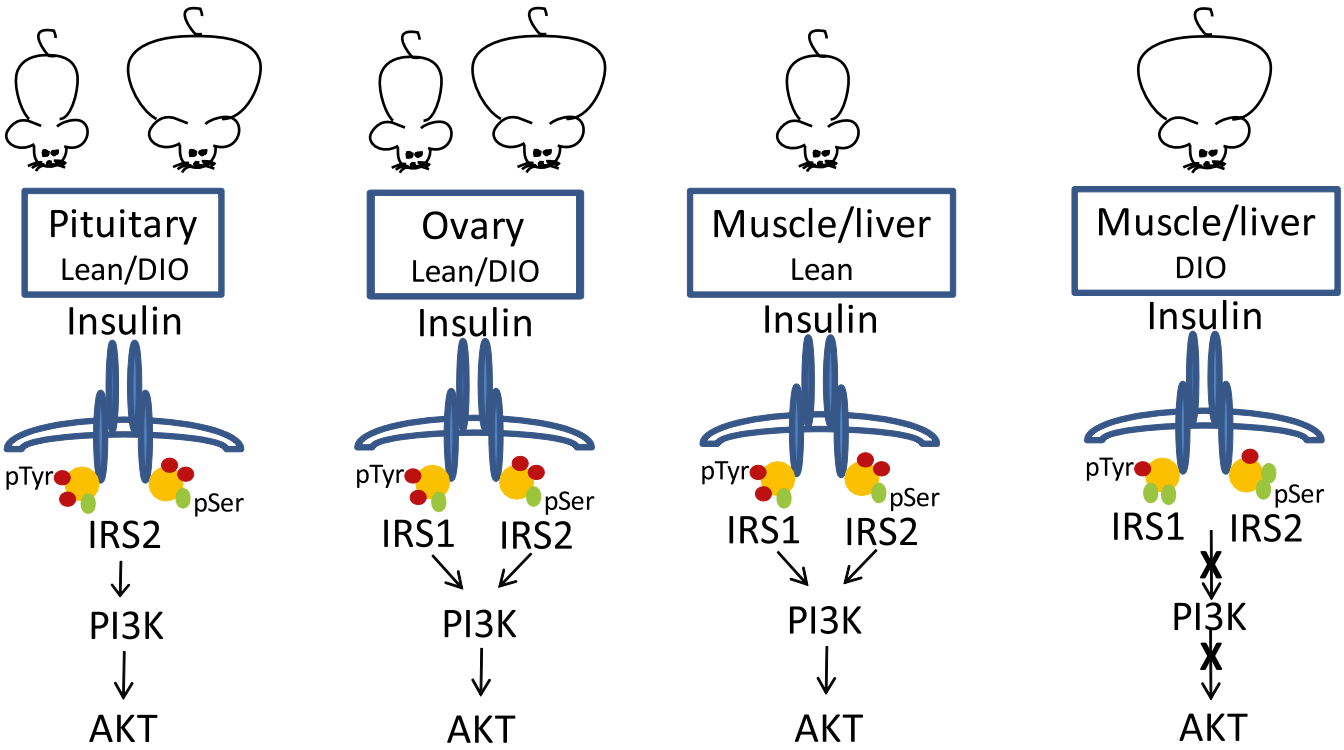

FIG. 8. A model summarizing the insulin-signaling pathways in the liver, muscle, and pituitary of lean or DIO mice. Arrows indicate active signaling pathways, and an X over the arrow indicates blocked signaling pathways. PI3K, PI 3-kinase.

ACKNOWLEDGMENTS

The authors acknowledge funding support from the Endocrine Fellow Foundation (to S.W.), the National Institutes of Health (NIH) (R01 HD44608 to A.W.), and the *Eunice Kennedy Shriver* National Institute of Child Health and Human Development/NIH through cooperative agreement (U54 HD41859) as part of the Specialized Cooperative Centers Program in Reproduction and Infertility Research. They also acknowledge NIH grant P60DK079637 (Diabetes Research Training Center [DRTC]).

No potential conflicts of interest relevant to this article were reported.

S.W. developed the project, researched data, and wrote the manuscript. S.D. contributed to the writing of the manuscript. F.W. helped plan the project. A.W. helped develop the project, performed some experiments, and wrote the manuscript.

The authors are grateful for the critical review of the manuscript by Dr. Sally Radovick (Johns Hopkins University).

REFERENCES

1. Ehrmann DA. Polycystic ovary syndrome. N Engl J Med 2005;352:1223–1236
2. Brothers KJ, Wu S, DiVall SA, et al. Rescue of obesity-induced infertility in female mice due to a pituitary-specific knockout of the insulin receptor. Cell Metab 2010;12:295–305
3. Burks DJ, Font de Mora J, Schubert M, et al. IRS-2 pathways integrate female reproduction and energy homeostasis. Nature 2000;407:377–382
4. Wu S, Divall S, Hoffman GE, Le WW, Wagner KU, Wolfe A. Jak2 is necessary for neuroendocrine control of female reproduction. J Neurosci 2011;31:184–192
5. Murata Y, Tsuruzoe K, Kawashima J, et al. IRS-1 transgenic mice show increased epididymal fat mass and insulin resistance. Biochem Biophys Res Commun 2007;364:301–307
6. Kiefer FW, Zeyda M, Gollinger K, et al. Neutralization of osteopontin inhibits obesity-induced inflammation and insulin resistance. Diabetes 2010;59:935–946
7. Hirosumi J, Tuncman G, Chang L, et al. A central role for JNK in obesity and insulin resistance. Nature 2002;420:333–336
8. White MF. IRS proteins and the common path to diabetes. Am J Physiol Endocrinol Metab 2002;283:E413–E422
9. White MF. Regulating insulin signaling and beta-cell function through IRS proteins. Can J Physiol Pharmacol 2006;84:725–737
10. Xu H, Barnes GT, Yang Q, et al. Chronic inflammation in fat plays a crucial role in the development of obesity-related insulin resistance. J Clin Invest 2003;112:1821–1830
11. Weisberg SP, McCann D, Desai M, Rosenbaum M, Leibel RL, Ferrante AW Jr. Obesity is associated with macrophage accumulation in adipose tissue. J Clin Invest 2003;112:1796–1808
12. Tanti JF, Jager J. Cellular mechanisms of insulin resistance: role of stress-regulated serine kinases and insulin receptor substrates (IRS) serine phosphorylation. Curr Opin Pharmacol 2009;9:753–762
13. Prada PO, Zecchin HG, Gasparetti AL, et al. Western diet modulates insulin signaling, c-Jun N-terminal kinase activity, and insulin receptor substrate-1 ser307 phosphorylation in a tissue-specific fashion. Endocrinology 2005;146:1576–1587
14. Divall SA, Williams TR, Carver SE, et al. Divergent roles of growth factors in the GnRH regulation of puberty in mice. J Clin Invest 2010;120:2900–2909
15. De Souza CT, Araujo EP, Bordin S, et al. Consumption of a fat-rich diet activates a proinflammatory response and induces insulin resistance in the hypothalamus. Endocrinology 2005;146:4192–4199
16. Fukuda M, Jones JE, Olson D, et al. Monitoring FoxO1 localization in chemically identified neurons. J Neurosci 2008;28:13640–13648
17. Tsuneki H, Murata S, Anzawa Y, et al. Age-related insulin resistance in hypothalamus and peripheral tissues of orexin knockout mice. Diabetologia 2008;51:657–667
18. Navratil AM, Song H, Hernandez JB, et al. Insulin augments gonadotropin-releasing hormone induction of translation in LbetaT2 cells. Mol Cell Endocrinol 2009;311:47–54
19. Kayampilly PP, Wanamaker BL, Stewart JA, Wagner CL, Menon KM. Stimulatory effect of insulin on 5alpha-reductase type 1 (SRD5A1) expression through an Akt-dependent pathway in ovarian granulosa cells. Endocrinology 2010;151:5030–5037
20. Munir I, Yen HW, Geller DH, et al. Insulin augmentation of 17alpha-hydroxylase activity is mediated by phosphatidylinositol 3-kinase but not extracellular signal-regulated kinase-1/2 in human ovarian theca cells. Endocrinology 2004;145:175–183
21. Goodarzi MO, Jones MR, Chen YD, Azziz R. First evidence of genetic association between AKT2 and polycystic ovary syndrome. Diabetes Care 2008;31:2284–2287
22. Seto-Young D, Avtanski D, Varadinova M, et al. Differential roles of MAPK-Erk1/2 and MAPK-p38 in insulin or insulin-like growth factor-I (IGF-I) signaling pathways for progesterone production in human ovarian cells. Horm Metab Res 2011;43:386–390
23. Lima MH, Souza LC, Caperuto LC, et al. Up-regulation of the phosphatidylinositol 3-kinase/protein kinase B pathway in the ovary of rats by chronic treatment with hCG and insulin. J Endocrinol 2006;190:451–459
24. Chakrabarty S, Nagamani M. Peripubertal hyperinsulinemia upregulates phosphatidylinositol 3-kinase/Akt pathway in rat ovaries. Reprod Sci 2008;15:274–284
25. Lawson MA, Jain S, Sun S, Patel K, Malcolm PJ, Chang RJ. Evidence for insulin suppression of baseline luteinizing hormone in women with polycystic ovarian syndrome and normal women. J Clin Endocrinol Metab 2008;93:2089–2096
26. Poretsky L, Glover B, Laumas V, Kalin M, Dunaif A. The effects of experimental hyperinsulinemia on steroid secretion, ovarian [^{125}I]insulin binding, and ovarian [^{125}I]insulin-like growth-factor I binding in the rat. Endocrinology 1988;122:581–585
27. Akamine EH, Marçal AC, Camporez JP, et al. Obesity induced by high-fat diet promotes insulin resistance in the ovary. J Endocrinol 2010;206:65–74
28. Sabio G, Kennedy NJ, Cavanagh-Kyros J, et al. Role of muscle c-Jun NH_2-terminal kinase 1 in obesity-induced insulin resistance. Mol Cell Biol 2010;30:106–115
29. Nakatani Y, Kaneto H, Kawamori D, et al. Modulation of the JNK pathway in liver affects insulin resistance status. J Biol Chem 2004;279:45803–45809
30. Belgardt BF, Mauer J, Wunderlich FT, et al. Hypothalamic and pituitary c-Jun N-terminal kinase 1 signaling coordinately regulates glucose metabolism. Proc Natl Acad Sci USA 2010;107:6028–6033
31. Diamanti-Kandarakis E, Argyrakopoulou G, Economou F, Kandaraki E, Koutsilieris M. Defects in insulin signaling pathways in ovarian steroidogenesis and other tissues in polycystic ovary syndrome (PCOS). J Steroid Biochem Mol Biol 2008;109:242–246
32. Bliss SP, Miller A, Navratil AM, et al. ERK signaling in the pituitary is required for female but not male fertility. Mol Endocrinol 2009;23:1092–1101
33. Fan HY, Liu Z, Shimada M, et al. MAPK3/1 (ERK1/2) in ovarian granulosa cells are essential for female fertility. Science 2009;324:938–941
34. Rice S, Christoforidis N, Gadd C, et al. Impaired insulin-dependent glucose metabolism in granulosa-lutein cells from anovulatory women with polycystic ovaries. Hum Reprod 2005;20:373–381
35. Nestler JE, Jakubowicz DJ, de Vargas AF, Brik C, Quintero N, Medina F. Insulin stimulates testosterone biosynthesis by human thecal cells from women with polycystic ovary syndrome by activating its own receptor and using inositolglycan mediators as the signal transduction system. J Clin Endocrinol Metab 1998;83:2001–2005
36. Duleba AJ, Pawelczyk LA, Yuen BH, Moon YS. Insulin actions on ovarian steroidogenesis are not modulated by metformin. Hum Reprod 1993;8:1194–1198
37. Barbieri RL. Insulin stimulates androgen accumulation in incubations of minced porcine theca. Gynecol Obstet Invest 1994;37:265–269
38. Dunaif A. Insulin resistance and the polycystic ovary syndrome: mechanism and implications for pathogenesis. Endocr Rev 1997;18:774–800
39. Poretsky L. On the paradox of insulin-induced hyperandrogenism in insulin-resistant states. Endocr Rev 1991;12:3–13
40. Codner E, Iñíguez G, Villarroel C, et al. Hormonal profile in women with polycystic ovarian syndrome with or without type 1 diabetes mellitus. J Clin Endocrinol Metab 2007;92:4742–4746
41. Micic D, Popovic V, Nesovic M, et al. Androgen levels during sequential insulin euglycemic clamp studies in patients with polycystic ovary disease. J Steroid Biochem 1988;31:995–999